Biochimica et Biophysica Acta 1853 (2015) 2086–2094

Contents lists available at ScienceDirect

Biochimica et Biophysica Acta

journal homepage: www.elsevier.com/locate/bbamcr

Ezrin interacts with the scaffold protein IQGAP1 and affects its cortical localization☆

Rathangadhara Chakrapani Nammalwar, Annika Heil, Volker Gerke *

Institute of Medical Biochemistry, Centre for Molecular Biology of Inflammation (ZMBE), Cells-in-Motion Cluster of Excellence (EXC 1003 — CiM), University of Münster, Von-Esmarch-Str. 56, 48149 Münster, Germany

ARTICLE INFO

Article history:
Received 25 September 2014
Received in revised form 18 December 2014
Accepted 19 December 2014
Available online 30 December 2014

Keywords:
Actin
Calcium-binding protein
Cell cortex
EF hand
Membrane

ABSTRACT

The cortical cytoskeleton constitutes an important subcellular structure that determines cell shape and regulates cell migration as well as membrane traffic to and from the plasma membrane. Many components of the cortical cytoskeleton have been identified including structural and scaffolding proteins, membrane–cytoskeleton linker proteins and signaling intermediates. We describe here an association of the membrane-F-actin linker protein ezrin with the scaffolding protein IQGAP1 that serves as a hub for concentrating different signaling complexes. Both, ezrin and IQGAP1 bind in a Ca^{2+}-dependent manner to the EF hand protein S100P and complexes consisting of Ca^{2+}-bound S100P, IQGAP1 and ezrin can be isolated by immunoprecipitation. Ezrin and IQGAP1 also interact in the absence of Ca^{2+}, thus independent of S100P. Direct ezrin–IQGAP1 interaction can be shown with the purified proteins. It is mediated via the N-terminal FERM domain of ezrin and the IQ domain of IQGAP1, respectively. Ezrin and IQGAP1 colocalize in the submembraneous cytoskeleton and in cellular protrusions of human epithelial cells and knockdown of ezrin reduces the cortical localization of IQGAP1. Thus, ezrin appears to participate in recruiting IQGAP1 to the cell cortex thereby establishing a close connection between membrane-F-actin contacts and actin regulators that can be assembled by IQGAP1. This article is part of a Special Issue entitled: 13th European Symposium on Calcium.

1. Introduction

Fundamental cellular processes such as differentiation, cell shape control, migration and intracellular trafficking require an active contribution of the cortical membrane-underlying cytoskeleton, a subcellular structure rich in actin filaments. Many components of the submembraneous cytoskeleton that interact with F-actin in a direct or indirect manner have been described and shown to play a role in conferring structural stability, membrane linkage and regulation of actin filament polymerization, branching and contractility (for review see [1]). These components include different myosins, actin bundling and crosslinking proteins, proteins that link actin filaments to the plasma membrane and regulators of actin polymerization and filament architecture, most prominently small GTPases of the Rho family and their downstream targets. Interactions between different components of the cortical cytoskeleton are manyfold, thereby enabling the assembly of a network structure that is highly flexible and can function both, as rigid scaffold in stable membrane extensions such as microvilli and stereocilia and as highly dynamic interface in filopodia, lamellipodia and membrane blebs that form in the course of cell migration (for recent reviews see [2–6]). However, although components of the cortical cytoskeleton have been studied extensively, the regulation of their assembly and disassembly is still not fully understood.

Ca^{2+} is an important signal known to trigger changes in the assembly and rigidity of the cell cortex [7] and several proteins transmitting transient Ca^{2+} elevations to downstream targets in the cortical cytoskeleton have been described. One class of Ca^{2+} binding proteins involved in this transduction of Ca^{2+} signals in the cell cortex is the S100 proteins, members of the EF hand superfamily. S100 proteins consist of two EF hand Ca^{2+}-binding motifs that are connected by a short linker and flanked by N- and C-terminal extensions of different length and sequence. As a general paradigm, S100 proteins transmit Ca^{2+} signals by interacting with and regulating specific effectors in their Ca^{2+} bound conformation and these effectors are thought to confer specificity to the respective S100 protein action (for review see [8–10]). S100P is a member of the family shown previously to bind and regulate two important components of the cortical cytoskeleton, ezrin and IQGAP1 [11]. Ezrin belongs to the ERM (ezrin–radixin–moesin) family of proteins that link plasma membrane-resident proteins to the cortical actin cytoskeleton. This linkage can occur via direct binding of the N-terminal ERM association domain (N-ERMAD; also called FERM for 4.1, ERM domain) to membrane proteins and the

☆ This article is part of a Special Issue entitled: 13th European Symposium on Calcium.

* Corresponding author at: Institute of Medical Biochemistry, Centre for Molecular Biology of Inflammation, University of Münster, Von-Esmarch-Str. 56, 48149 Münster, Germany. Tel.: +49 2518356722; fax: +49 2518356748.
E-mail address: gerke@uni-muenster.de (V. Gerke).

http://dx.doi.org/10.1016/j.bbamcr.2014.12.026
0167-4889/

C-ERMAD to F-actin. However, the linker function needs to be activated because ezrin and the other ERM proteins reside in an autoinhibited conformation in non-stimulated cells (for review see [13]). Ca^{2+}-triggered binding of S100P to the N-ERMAD can relieve the autoinhibition and thereby activate ezrin's function in, e.g. cell migration [15]. IQGAP1, on the other hand, is a multidomain scaffolding protein of the cell cortex that can recruit many interaction partners and thereby act in signal transduction pathways and the regulation of actin cytoskeleton and microtubule dynamics (for reviews see [16,17]). S100P binding to IQGAP1, which is also Ca^{2+} dependent, has been shown to alter signal transduction properties of IQGAP1, specifically the binding of B-Raf and activation of MEK1/2 occurring in response to EGF treatment [12]. Although IQGAP1 has not been shown to participate directly in physical membrane–cytoskeleton linkage, it has been reported that it can associate with FERM domain containing proteins such as protein 4.1R [16,18]. Moreover, a proteomic approach employing the internal repeat region of IQGAP1 as a bait recently identified ezrin, radixin and moesin as interacting proteins suggesting a link between IQGAP1 and ERM proteins [19].

A link between IQGAP1 and ezrin could also be established by S100P that can interact directly with both, ezrin and IQGAP1. Therefore, we herein investigated whether complexes consisting of S100P, ezrin and/or IQGAP1 can exist in cells. Such complexes could provide a means to physically connect ezrin's membrane-F-actin linking activity with regulators of the actin cytoskeleton such as Cdc42, Rac1 and Dia1 that can be recruited by IQGAP1. We show that S100P, IQGAP1 and ezrin can indeed be precipitated together from cell lysates in a Ca^{2+} dependent manner. Interestingly, upon extending our analyses to the Ca^{2+} regulation of complex formation we observed that an interaction between ezrin and IQGAP1 can also occur in the absence of Ca^{2+} and S100P. This interaction is direct, is mediated by the N-ERMAD and IQ domain of ezrin and IQGAP1, respectively, and is in line with a colocalization of both proteins in the cortex of human epithelial cells. Furthermore, siRNA-mediated depletion experiments reveal that ezrin is required for an efficient cortical localization of IQGAP1 in these cells. Thus, our results identify a direct interaction between ezrin and the IQ domain of IQGAP1 that could be of importance for connecting the IQGAP1-mediated cortical assembly of actin regulators to the membrane-F-actin linkage provided by ezrin.

2. Materials and methods

2.1. Cell culture and transfection

HeLa and HEK293T cells were maintained in Dulbecco's modified Eagle's medium supplemented with 10% fetal calf serum (FCS), 2 mM L-glutamine, and antibiotics in a 7% CO_2 incubator at 37 °C. For EGF stimulation experiments, HeLa were first starved by cultivation in serum free medium for 16 h. Subsequently, EGF was added to a final concentration of 50 ng/ml and cultivation was continued for the times indicated. Human urinary bladder carcinoma (ECV304) cells were maintained in Earle's 199 medium supplemented with 10% fetal calf serum (FCS), 2 mM L-glutamine, and antibiotics in a 5% CO_2 incubator at 37 °C. *Spodoptera frugiperda* 9 (SF9) insect cells were cultured in TC-100 medium with 10% FCS and 0.26% tryptose phosphate broth (Sigma) at 27 °C in air atmosphere. Cells were transiently transfected using Lipofectamine 2000 (Invitrogen) according to the manufacturer's instructions unless stated otherwise. Transient siRNA transfections to down-regulate ezrin were performed using siGENOME SMART pool human ezrin siRNA (Dharmacon). Transfections were performed using Lipofectamine-2000 (Invitrogen) according to manufacturer's instructions.

2.2. Plasmids

pCantag-IQGAP1 full length and pCDNA3.1 plasmids encoding different domains of human IQGAP1 were generated as described [20]. Constructs encoding His-tagged versions of the N-ERMAD and C-ERMAD of human ezrin in pET-28a as well as the GFP–S100P plasmid have been described previously [11].

2.3. Recombinant protein expression and purification

Expression and purification of full length GST–IQGAP1 from SF9 insect cells infected with *Autographa californica* nuclear polyhedrosis baculoviruses was performed as described [12]. GST-tagged N-ERMAD, $(His)_6$-tagged S100P was purified from *Escherichia coli* cells (strain BL21(DE3)pLysS) as described earlier [12].

$(His)_6$-tagged N- or C-ERMAD was expressed in *E. coli* cells (strain BL21(DE3)pLysS). Transformed bacteria were grown to an OD_{600} of 0.6 at 37 °C, and recombinant protein expression was then induced by adding isopropyl β-D-1-thiogalactopyranoside to a final concentration of 1 mM. After incubation for 3 h at 37 °C, cells were harvested by centrifugation (2500 ×*g*; 10 min) and resuspended in lysis buffer (40 mM Hepes, pH 7.4, 20 mM imidazole, pH 7.4, 300 mM NaCl, 1 mM EDTA, 10 mM β-mercaptoethanol, 1 mM PMSF). Cells were lysed by three freeze/thaw cycles and sonication (duty cycle 50%, output control 5′), and the remaining cellular debris was removed by centrifugation for 1 h at 100,000 ×*g*. The supernatant obtained after the ultracentrifugation step was applied to a Ni–NTA-agarose column equilibrated with lysis buffer. After washing with washing buffer (40 mM Hepes, pH 7.4, 150 mM NaCl, 10 mM β-mercaptoethanol, 1 mM PMSF) containing increasing concentrations of imidazole (25 and 35 mM), His-tagged-N- or C-ERMAD was eluted with this buffer supplemented with 250 mM imidazole.

2.4. In vitro transcription/translation

[^{35}S]-methionine labeled IQGAP1 full length and domains were expressed using the TnT® Quick-coupled transcription/translation system (Promega, Madison, WI). 50 μL reaction mixture contained 1 μg of pCDNA construct encoding the respective IQGAP1 derivative (full-length or mutant), 9 μCi of [^{35}S] methionine (GE-Healthcare) and 40 μL of TnT® Quick Master Mix. This mixture was incubated at 30 °C for 90 min. 10% of the mixture was subjected to SDS-PAGE and autoradiography to confirm the proper translation and labeling and the remaining 45 μL was used in the in vitro interaction assays.

2.5. In vitro interaction assays

In vitro binding assays were performed using a column-based affinity chromatography approach. To analyze the interaction of IQGAP1 and ezrin, glutathione-Sepharose 4B (GE Healthcare) beads containing 3 μg of immobilized GST–IQGAP1 or GST alone as control were equilibrated in buffer A (40 mM Hepes, pH 7.4, 20 mM imidazole, pH 7.4, 150 mM NaCl, 1 mM DTT, 1.5 mM PMSF). 30 μg of His-tagged N- or C-ERMAD protein was dialyzed against the equilibration buffer and added in the fluid phase. After incubation at 4 °C for 1 h and washing with the same buffer, the protein complexes were eluted with 40 mM Hepes, pH 7.4, and 100 mM GSH. Fractions of the flow-through and of washing and elution steps were collected and analyzed by SDS-PAGE and Western blots employing monoclonal mouse anti-GST (B14, Santa Cruz Biotechnology, Heidelberg, Germany) and monoclonal mouse anti-His antibodies (Qiagen, Hilden, Germany) followed by a goat anti-mouse POX labeled secondary antibodies (Dianova, Hamburg, Germany).

For further mapping of the N-ERMAD binding domain on IQGAP1, equivalent amounts of purified GST-tagged N-ERMAD and GST alone (control) were immobilized to glutathione-Sepharose 4B (GE Healthcare) beads in buffer A. A small aliquot of protein-immobilized resin was subjected to SDS-PAGE and stained with Coomassie Brilliant Blue or probed by immunoblotting to ensure that equal amounts of proteins were used. In vitro translated, [^{35}S]-methionine-labeled IQGAP1

full length or domains were added to the immobilized GST–N-ERMAD and incubated overnight at 4 °C. After washing with the respective binding buffers, bound proteins were eluted with boiling SDS sample buffer and analyzed by SDS-PAGE and autoradiography.

2.6. Co-immunoprecipitation and pulldown experiments

Control or GFP–S100P overexpressing HeLa cells of a 100 mm culture dish were washed once with PBS and scraped into 0.5 ml of lysis buffer (20 mM imidazole, pH 6.8, 100 mM NaCl, 1% Triton-X-100, 0.04% NaN_3 and Complete protease inhibitor mixture (Roche Diagnostics)) containing either 0.5 mM $CaCl_2$ or 2 mM EGTA. Cell lysis was performed on an overhead shaker for 30 min at 4 °C followed by centrifugation (300 ×*g*, 30 min, 4 °C). 3 mg of total protein of the resultant post-nuclear supernatant (PNS) was applied to protein A-Sepharose Cl-4B (GE Healthcare) equilibrated in lysis buffer either together with a polyclonal rabbit anti-IQGAP1 antibody (H-108, Santa Cruz Biotechnology) or nonspecific polyclonal rabbit IgGs (DAKO, Glostrup, Denmark). After incubation for 2 h or overnight at 4 °C and washing with the respective lysis buffer, bound proteins were eluted with boiling SDS sample buffer. Samples of the PNS and the eluted proteins were analyzed by SDS-PAGE and Western blot using monoclonal anti-IQGAP1 antibodies diluted 1:5000 (BD Biosciences) and polyclonal rabbit anti-ezrin antibodies diluted 1:5000 (Upstate Biotechnology, Inc., Lake Placid, NW) or monoclonal mouse anti-ezrin antibodies diluted 1:250 (BD Transduction laboratories, Heidelberg, Germany) followed by the respective POX-labeled secondary antibodies or infrared-labeled Odyssey® secondary antibodies (LI-COR Biosciences, Germany).

Relative amounts of ezrin co-immunoprecipitated with IQGAP1 in Ca^{2+} and EGTA conditions were quantified in relation to the precipitated IQGAP1 by densitometry using ImageJ. For this purpose, amounts of co-precipitated ezrin from three independent co-IP experiments were compared to the corresponding amount of IQGAP1.

2.7. Pulldown of ezrin and IQGAP1 from HeLa lysates using purified S100P

Pulldown experiments of His-tagged S100P wild type with endogenous ezrin and IQGAP1 from HeLa cell lysates employed 5 μg of purified S100P wild type protein that was immobilized to Ni–NTA-agarose (Macherey Nagel, Germany) beads. HeLa cells grown on a 100 mm culture dish were scraped into lysis buffer (10 mM Hepes, pH 7.4, 150 mM NaCl, 1% Triton X-100, 2 mM HEDTA, and Complete protease inhibitor mixture (Roche Diagnostics)) containing either 500 μM $CaCl_2$ or 10 μM $ZnSO_4$. Lysis was performed on an overhead shaker for 30 min at 4 °C followed by centrifugation (300 ×*g*, 30 min, 4 °C). 3 mg of total protein from the resulting supernatant (PNS) was then applied to immobilized S100P. After incubation on an overhead shaker overnight at 4 °C and washing with lysis buffer, bound proteins were eluted with boiling SDS sample buffer. Samples of the PNS and the eluted proteins were analyzed by SDS-PAGE and Western blot using monoclonal mouse anti-IQGAP1 antibodies diluted 1:5000 (BD Biosciences), polyclonal rabbit anti-ezrin antibodies diluted 1:5000 (Upstate Biotechnology, Inc., Lake Placid, NW) and monoclonal mouse anti-6×His epitope antibodies diluted 1:100 (Thermo Scientific) followed by the respective infrared-labeled Odyssey® secondary antibodies (LI-COR Biosciences, Germany).

2.8. Immunofluorescence analysis

Cells grown on fibronectin-coated coverslips were fixed with 3% formaldehyde in PBS for 6 min at room temperature. Cells were then subjected to permeabilization with 0.5% Triton-X-100 for 15 min and quenching with NH_4Cl for 15 min. Following treatment with 2% BSA in PBS for 1 h, cells were incubated with rabbit polyclonal anti-IQGAP1 antibodies diluted 1:1000 (Santa Cruz Biotechnology) and mouse monoclonal anti-ezrin antibodies diluted 1:100 (clone 18, BD biosciences) overnight at 4 °C. Primary antibodies were detected with Alexa Fluor 488 goat anti-rabbit (diluted 1:400) (Invitrogen) and Alexa Fluor 568 donkey anti-mouse diluted (1:200) (Invitrogen) secondary antibodies. Stained cells were mounted in Mowiol and analyzed using a confocal laser scanning microscope (LSM 780; Zeiss, Jena, Germany).

2.9. Quantification of cortical IQGAP1 staining

To quantify the levels of cortical IQGAP1 enrichment, control and ezrin downregulated ECV304 cells were imaged using exactly the same confocal laser scanning parameters. Cortical IQGAP1 enrichment was quantified using ImageJ. Therefore, the raw integrated density of IQGAP1 from a defined cortical region was divided by the raw integrated density of total cellular IQGAP1. This yielded the percentage cortical enrichment relative to the total cellular IQGAP1. The mean relative enrichment in 30 control cells was then compared to the mean relative enrichment in the same number of ezrin depleted cells.

2.10. Statistical analysis

Unpaired, two-tailed Student's t test was applied to determine if the mean relative cortical enrichment of IQGAP1 in ezrin downregulated ECV304 cells was significantly decreased as compared to that of control transfected cells. $P < 0.05$ was considered as significant.

3. Results and discussion

3.1. Identification of S100P–IQGAP1–ezrin complexes

Our previous biochemical work identified S100P–ezrin and S100P–IQGAP1 complexes that only form in the presence of Ca^{2+}, i.e. require the Ca^{2+}-bound conformation of S100P [11,12]. In these complexes the binding sites on S100P map to different regions. Whereas the C-terminal extension encompassing residues 87 to 95 harbors the ezrin binding site [15], residues 21–25 in the N-terminal EF hand are required for IQGAP1 binding [12]. This suggests that S100P can simultaneously bind to ezrin and IQGAP1 although such simultaneous complex formation had not been shown before. To address this we carried out pulldown experiments with His-tagged S100P that was immobilized on Ni–NTA beads and incubated with HeLa cell lysates containing endogenous ezrin and IQGAP1. Fig. 1 reveals that S100P can pulldown both ezrin and IQGAP1 from the lysates in the presence of Ca^{2+}. S100B, another member of the S100 protein family, had also been shown to bind IQGAP1 and in this case the interaction was observed

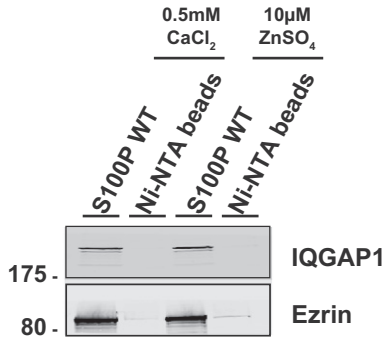

Fig. 1. Pulldown of ezrin and IQGAP1 by S100P. 3 mg of protein from a post nuclear supernatant (PNS) of HeLa cells lysed in the presence of 0.5 mM $CaCl_2$ or 10 μM $ZnSO_4$ was applied to Ni–NTA agarose containing immobilized 5 μg S100P wildtype (WT). After washing with lysis buffer containing either Ca^{2+} or Zn^{2+}, the remaining column-bound protein complexes and the PNS were subjected to Western blot analysis using monoclonal anti-IQGAP1 (dilution 1:5000) and polyclonal anti-ezrin (1:5000) antibodies. Lanes 2 and 4 depict control experiments employing Ni–NTA agarose beads alone. The blot shows a representative example of 3 independent experiments.

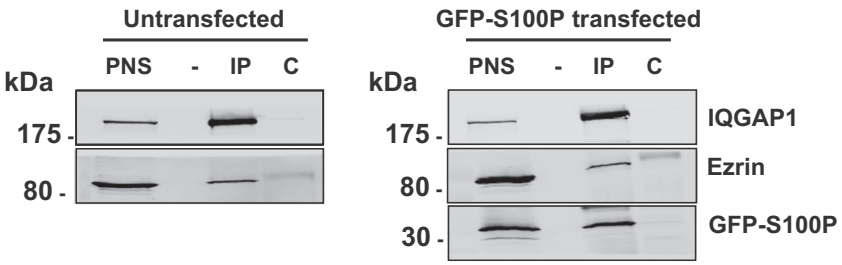

Fig. 2. Co-immunoprecipitation of ezrin and IQGAP1 in the presence of S100P. Untransfected or pEGFP–S100Pwt-transfected HeLa cells were lysed 24 h post transfection in the presence of 0.5 mM $CaCl_2$. 3 mg of protein of a post nuclear supernatant (PNS) prepared from the lysates was subjected to immunoprecipitation using 5 μg of polyclonal anti-IQGAP1 antibodies (IP) or nonspecific polyclonal IgGs as control (C). The PNS and the precipitated proteins were subjected to 12% SDS-PAGE and Western blot analysis was performed using monoclonal anti-IQGAP1 (1:5000), monoclonal anti-ezrin (1:250) and monoclonal anti-GFP (1:1000) antibodies. Blot shows a representative example of 3 independent experiments.

both, in the presence of Ca^{2+} and in the presence of Zn^{2+} [20]. Therefore, we also determined whether Zn^{2+} can trigger an interaction between S100P and ezrin/IQGAP1 by performing the pulldowns in the presence of Zn^{2+} instead of Ca^{2+}. As shown in Fig. 1, a pulldown of ezrin and IQGAP1 by S100P is also observed in the presence of Zn^{2+}, most likely because Ca^{2+} and Zn^{2+} binding to S100P both induce the interaction-competent conformation. The divalent cations, Ca^{2+} and Zn^{2+}, are essential to establish the S100P interactions with ezrin and IQGAP1 as no pulldown is observed in the presence of EGTA (not shown). Because S100P can form heterodimers with S100A1 [21] and S100B forms heterodimers with S100A1 [22], we also analyzed whether S100B is present in the S100P pulldowns. However, we were not able to

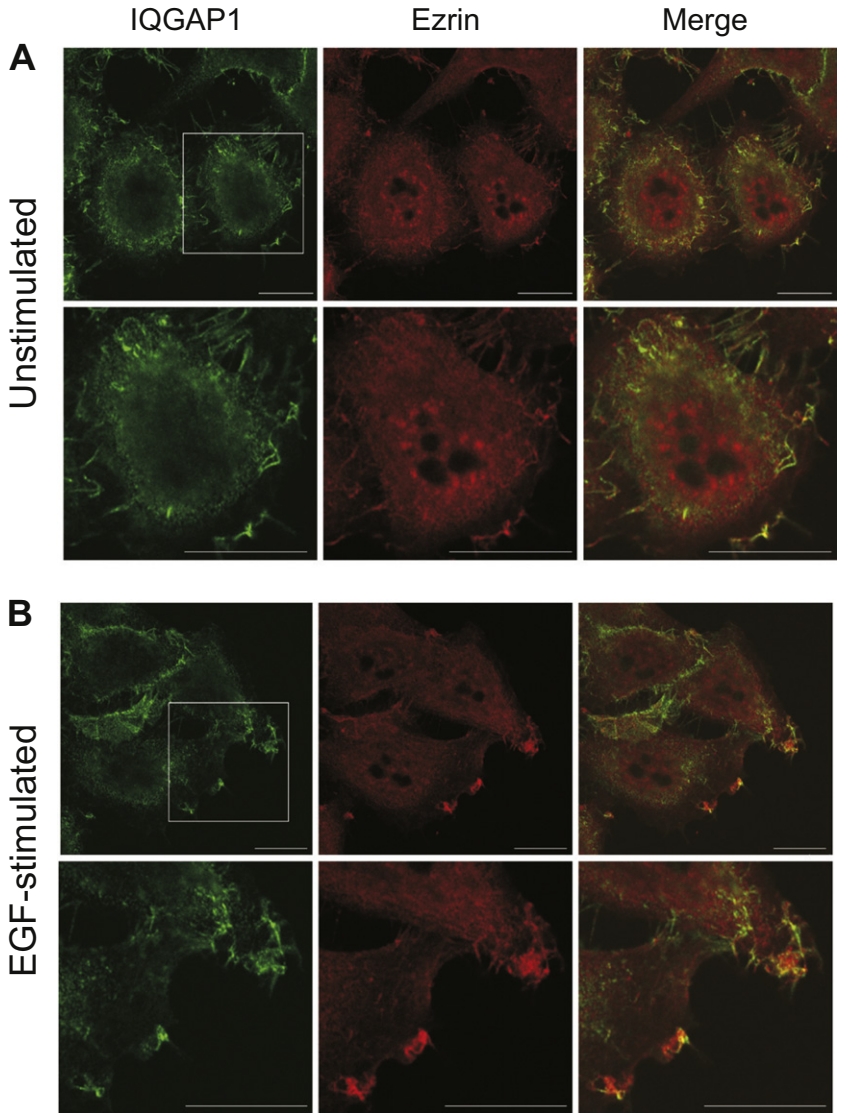

Fig. 3. Colocalization of ezrin and IQGAP1 in HeLa cells. HeLa cells were serum-starved for 16 h and either kept unstimulated (A) or were stimulated with 50 ng/ml EGF for 5 min (B). After fixation and permeabilization, cells were stained with polyclonal antibodies against human IQGAP1 (1:1000) (*green channel*) and monoclonal antibodies against human ezrin (1:100) (*red channel*) followed by appropriate fluorescently labeled secondary antibodies. The lower panels show higher magnifications of the boxed areas. Scale bars, 10 μm.

detect any specific S100B band in the S100P pulldowns, neither in the presence of Ca^{2+} nor in the presence of Zn^{2+} (not shown). Collectively, the pulldowns indicate that Ca^{2+} and Zn^{2+} can trigger interactions of S100P with ezrin and IQGAP1 and that ezrin and IQGAP1 do not effectively compete with one another for S100P binding. While this suggests that S100P can simultaneously bind ezrin and IQGAP1, we cannot formally exclude that our pulldown approach enriches independently formed S100P/ezrin and S100P/IQGAP1 complexes.

Next, we employed co-immunoprecipitation (co-IP) experiments to verify that S100P–IQGAP1–ezrin complex formation can also occur within cells. Due to the lack of highly specific antibodies against S100P these experiments were carried out with HeLa cells ectopically expressing GFP–S100P. As shown in Fig. 2, both ezrin and GFP–S100P can be co-immunoprecipitated with anti-IQGAP1 antibodies in the presence of Ca^{2+} indicative of intracellular interactions probably resembling a tripartite complex. Interestingly, control experiments revealed an efficient co-IP of IQGAP1 and ezrin also in non-transfected cells (Fig. 2). Immunofluorescence analysis was next employed to analyze whether IQGAP1 and ezrin also colocalize within cells. Therefore, HeLa cells were either left unstimulated or stimulated with EGF to raise intracellular Ca^{2+} levels and then fixed and stained with anti-IQGAP1 and anti-ezrin antibodies. Whereas both proteins show some general cytoplasmic distribution, a significant enrichment is seen at sites close to the plasma membrane, in particular in membrane protrusions and membrane ruffles (Fig. 3). This cortical colocalization of IQGAP1 and ezrin is already evident in unstimulated cells.

3.2. IQGAP1 and ezrin interact directly

Prompted by the above results, in particular the observation that the degree of co-IP of IQGAP1 and ezrin is not affected significantly by the ectopic expression of GFP–S100P and that both proteins colocalize to some extent in unstimulated cells at resting Ca^{2+} levels, i.e. without activation of S100P (Figs. 2 and 3), we analyzed whether IQGAP1 and ezrin can interact with one another independent of Ca^{2+}-bound S100P. Therefore, a co-IP of IQGAP1 and ezrin was carried out in the presence and absence of elevated Ca^{2+} levels. Fig. 4 reveals that an efficient co-IP is observed also in the absence of Ca^{2+}, although the relative amount of co-precipitated ezrin is higher in the presence as compared to the absence of Ca^{2+}. Thus, it appears that IQGAP1–ezrin complexes can form independently of active, Ca^{2+}-bound S100P and that S100P can increase this complex formation in response to Ca^{2+} elevation. In line with the colocalization of both proteins in unstimulated HeLa cells, the efficient co-IP of IQGAP1 and ezrin is not significantly affected by EGF stimulation (Fig. 4). This indicates that a complex consisting of IQGAP1 and ezrin can form even in resting cells, i.e. probably without

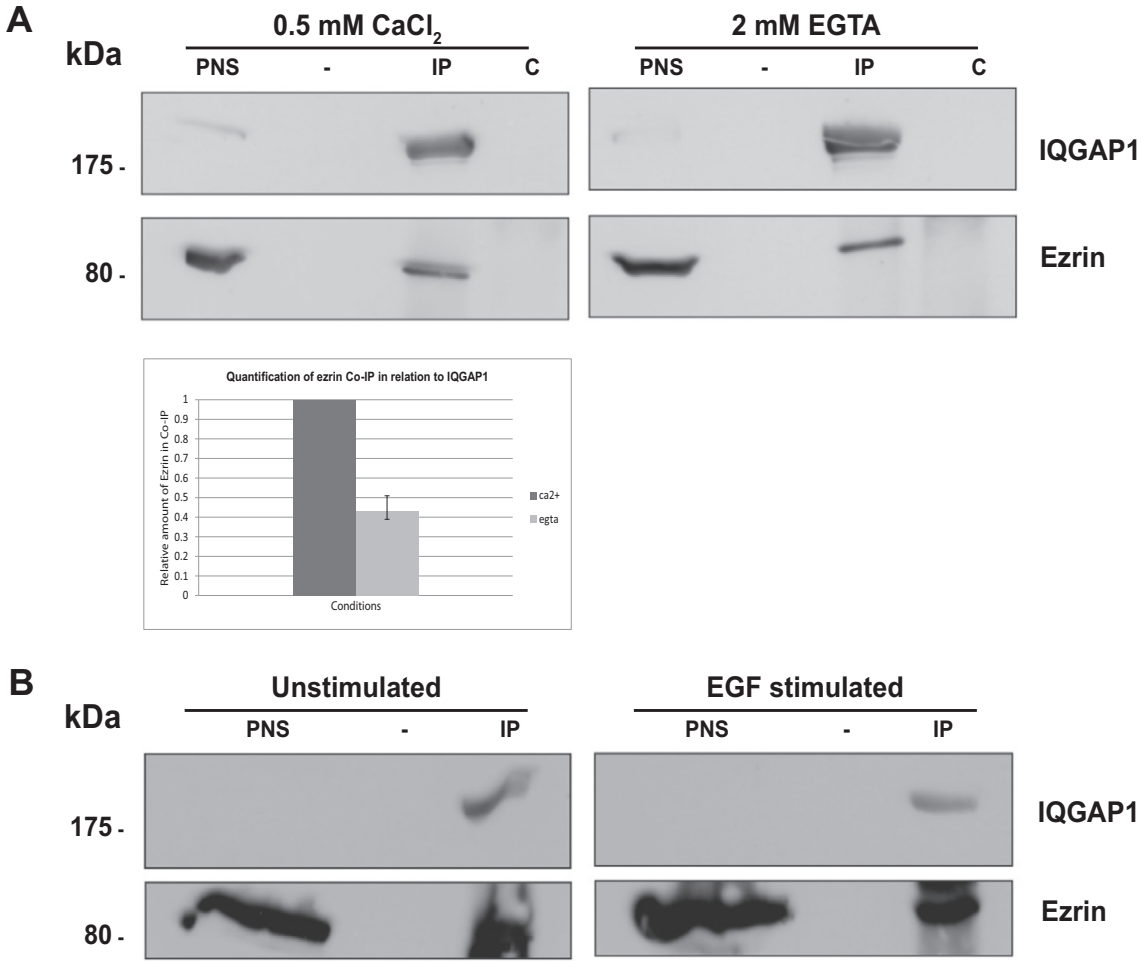

Fig. 4. Ezrin and IQGAP1 interact independently of Ca^{2+}-S100P. A. HeLa cells were lysed in the presence or absence (2 mM EGTA) of Ca^{2+} and 3 mg of protein of a post nuclear supernatant (PNS) prepared from these lysates were subjected to immunoprecipitation using 5 μg of polyclonal anti-IQGAP1 antibodies (IP) or nonspecific polyclonal IgGs (control, C). The PNS and the precipitated proteins were analyzed by Western blot using monoclonal anti-IQGAP1 (1:5000) and polyclonal anti-ezrin antibodies (1:5000). A (*bar graph*). The relative amount of ezrin in the co-IP carried out in 0.5 mM $CaCl_2$ and 2 mM EGTA was compared to the corresponding amount of IQGAP1. Quantification was achieved by densitometry as described in the Materials and methods. B. HeLa cells were serum starved for 16 h and either kept unstimulated or were stimulated with 50 ng/ml EGF for 5 min before cell lysis. Equal amounts of the PNS prepared from the respective cell lysates were further processed as described in A.

full activation of the autoinhibited ezrin. However, as colocalization of the two proteins appears to be restricted to areas of membrane protrusions that usually contain activated ezrin (Fig. 3), it remains possible that the resting HeLa cells employed in our analysis contain enough active, membrane-recruited ezrin that could establish an interaction in the cell cortex. Future experiments have to reveal to what extent dormant, autoinhibited ezrin can indeed bind IQGAP1.

As such co-IP of IQGAP1 and ezrin had not been reported before, we explored the S100-independent IQGAP1–ezrin association in more detail. While co-IP is indicative of an association, it does not show that the two proteins interact directly. To address the question of direct interaction we performed binding experiments using purified proteins. A first series of experiments employed the two major protein interaction domains of ezrin to also map a potential IQGAP1 binding site in the ezrin molecule. N-ERMAD and C-ERMAD were expressed as His-tagged fusions, purified and applied to glutathione-Sepharose columns containing either purified GST-tagged IQGAP1 or GST alone as control. Bound proteins were then eluted with reduced glutathione to release the column-bound GST-protein (GST–IQGAP1 or GST) and any interacting ezrin derivative. While a direct interaction was observed for N-ERMAD, no interaction of C-ERMAD with immobilized GST–IQGAP1 could be seen (Fig. 5). The binding was specific for IQGAP1 as immobilized GST alone did not show an interaction with N-ERMAD. Thus, IQGAP1 and ezrin can interact directly and the binding site is located in the N-terminal ERM association domain of ezrin. This domain also harbors the binding sites for different membrane proteins, the membrane lipid phosphatidylinositol (4,5)-bisphosphate (PIP_2) and S100P (for review see [14]).

Next, we mapped the ezrin binding site on IQGAP1 by employing in vitro translated IQGAP1 mutant derivatives and immobilized GST–N-ERMAD. In a first set of experiments we could show that N-ERMAD binds to the N-terminal part of IQGAP1 encompassing the CHD, IR, WW and IQ domains (Fig. 6). Thus, we next employed IQGAP1 mutants comprising different combinations of these domains and analyzed their capability of N-ERMAD binding in the pulldown assay. Fig. 6 shows that all mutant derivatives containing the IQ domain bind to immobilized N-ERMAD, whereas those lacking the IQ domain did not interact. Furthermore, a truncated derivative solely encompassing residues 745–862 and thus the four IQ motifs of the IQ domain also interacted with N-ERMAD (Fig. 6). Collectively, these binding studies show that ezrin and IQGAP1 can interact directly with one another and that the binding sites for this interaction map to the N-ERMAD and IQ domains, respectively.

The IQ domain of IQGAP1 harbor interaction sites for several other proteins including calmodulin and S100P [16,12] and it remains to be determined whether and to what extent these protein interactions interfere with one another. Using a proteomic approach and the IQGAP-specific internal repeat (IR) sequences as a bait, an interaction of these repeats with the FERM domain of ERM proteins has been reported recently [19]. However, the mode of interaction appears to be different from the IQ domain-mediated ezrin binding seen in our experiments as (1) the repeat-mediated binding is not seen for the non-activated ezrin and (2) we do not observe an interaction of N-ERMAD with the IR region of IQGAP1 in our experimental setup (Fig. 6). We have no experimentally substantiated explanation for these discrepant findings concerning the IQGAP1–ezrin interaction site but think that the different observations might be due to the different constructs used. Whereas [19] employed the IR region as an isolated domain, we used longer domain constructs (Fig. 6) or full-length IQGAP1 (Fig. 5). Thus, an interaction of N-ERMAD with the IR region might be masked in, e.g., the IR-WW constructs and therefore escaped detection in our approach.

3.3. Ezrin depletion affects the IQGAP1 distribution in human epithelial ECV304 cells

Given the direct interaction of ezrin and IQGAP1 seen in pulldown and co-IP experiments we next wanted to analyze whether this interaction plays a role in determining the cortical localization of the proteins. IQGAP1 had been shown previously to localize to the submembranous cytoskeleton of various cells and a recent report could identify the membrane skeleton protein 4.1R as an interaction partner that is involved in directing IQGAP1 to the leading edge of human epithelial ECV304 cells during wound closure migration [18]. Because ezrin shares some homology with protein 4.1R in the N-ERMAD domain, we also employed these cells to analyze whether ezrin plays a role in determining a cortical localization of IQGAP1. Fig. 7A reveals that, similar to HeLa cells, ECV304 cells also show an enrichment of both, ezrin and IQGAP1 at or close to the plasma membrane. Next, we depleted the ECV304 cells of ezrin by employing specific siRNAs and analyzed the effect on IQGAP1 distribution. An efficient knockdown of ezrin could be achieved as revealed by Western blot as well as immunofluorescence analysis and this knockdown did not affect the total level of IQGAP1 (Fig. 7B and C). The localization of IQGAP1 in the ezrin knockdown cells was then analyzed by immunofluorescence microscopy and compared to that of cells transfected with control siRNA. As shown in Fig. 7C, a significant reduction of cortical IQGAP1 staining is observed in the ezrin-depleted cells indicative of a role of ezrin in establishing an enrichment of IQGAP1 in the cell cortex of ECV304 cells.

Because cortical colocalization of ezrin and IQGAP1 is already seen in unstimulated HeLa and ECV304 cells, we believe that full activation of ezrin by phosphorylation of Thr-567 occurring downstream of stimulated growth factor receptors is not necessary to establish an IQGAP1 binding-competent ezrin conformation. Non-phosphorylated ezrin can bind the plasma membrane lipid PIP_2 [23] and thus can also be targeted to the plasma membrane via lipid binding [24]. Most likely, such membrane-bound ezrin could in turn recruit IQGAP1 to submembranous sites via the direct interaction described here. Upon intracellular Ca^{2+} elevation, for example in response to growth factor stimulation, Ca^{2+}-bound S100P could then be directed to the cortical

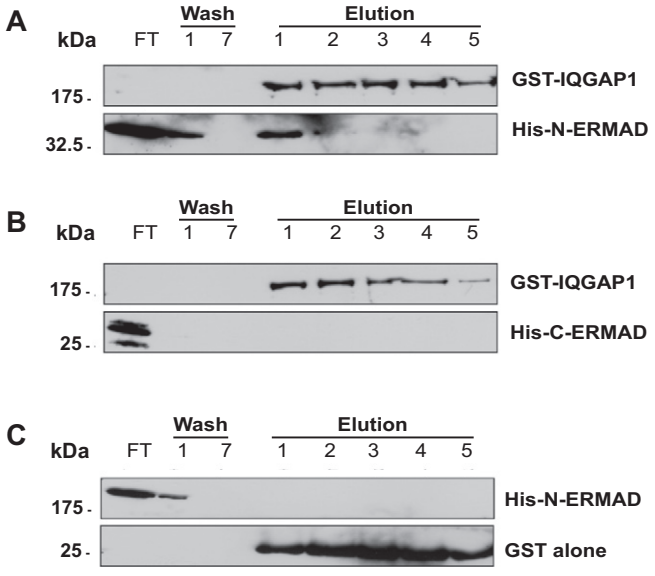

Fig. 5. IQGAP1 interacts directly with the N-terminal ERM association domain of ezrin. Representative results of three independent affinity chromatography approaches with purified proteins. Equal amounts of $(His)_6$-tagged N-ERMAD (A) or C-ERMAD (B) were loaded onto glutathione-Sepharose columns containing immobilized GST–IQGAP1 or, as exemplified for N-ERMAD, onto columns containing GST alone (C). After several washing steps, protein complexes were eluted by applying a buffer containing reduced glutathione. Eluted fractions were subjected to Western blot analysis using monoclonal anti-$(His)_6$, anti-IQGAP1 or anti-GST antibodies. The lower part of panel A shows some unspecific background not coinciding with protein bands. The double band of His-CERMAD seen in the flow through in panel B is most likely due to proteolysis.

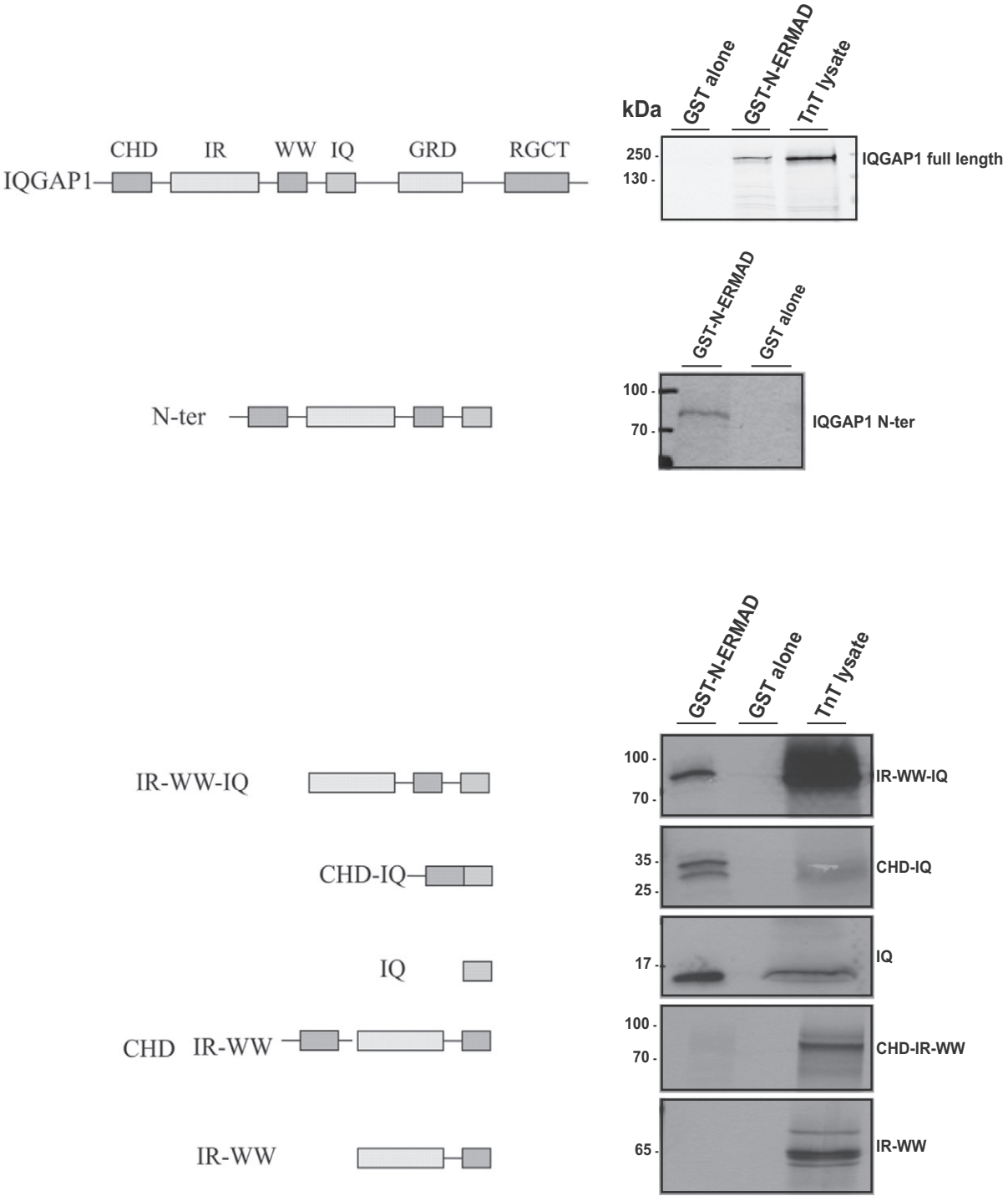

Fig. 6. N-ERMAD binds to the IQ domain of IQGAP1. Schematic overviews of full length IQGAP1 and its mutant derivatives which were tested for N-ERMAD binding are represented on the left hand side. The corresponding results of in-vitro interaction experiments are on the right. [^{35}S]-methionine-labeled full-length IQGAP1 protein as well as the mutants comprising different domains were translated in vitro. Subsequently, they were loaded onto glutathione-Sepharose beads containing immobilized GST–N-ERMAD or GST alone (control) in the absence of Ca^{2+}. After washing several times, the bound protein complexes as well as the lysate from the respective in vitro expression (TnT lysate) were subjected to SDS-PAGE followed by autoradiography. Note that full length IQGAP1 and all the mutants containing the IQ domain (including the IQ domain alone) bound to GST–N-ERMAD. The double bands seen in case of CHD–IQ and IR–WW are most likely the result of some proteolysis occurring during expression or pulldown. Abbreviations used are as follows: CHD, calponin homology domain; IR, internal repeats; WW, domain with two conserved Trp (W) residues; IQ, IQ domain containing 4 IQ motifs; GRD, GAP related domain; RGCT, Ras-GAP C-terminus.

IQGAP1/ezrin complexes and possibly recruit additional ezrin and/or IQGAP1 molecules and stabilize an activated ezrin conformation (Fig. 8). The close apposition of IQGAP1 and ezrin in such complexes could establish a physical link between membrane-F-actin attachment sites provided by ezrin and signaling molecules regulating actin dynamics such as Cdc42 and Rac1 that are recruited by IQGAP1. As a consequence, specific actin modulation can be targeted to membrane–actin contact sites. Future experiments have to reveal whether such close proximity indeed exists and also involves downstream effectors of Cdc42 and Rac1.

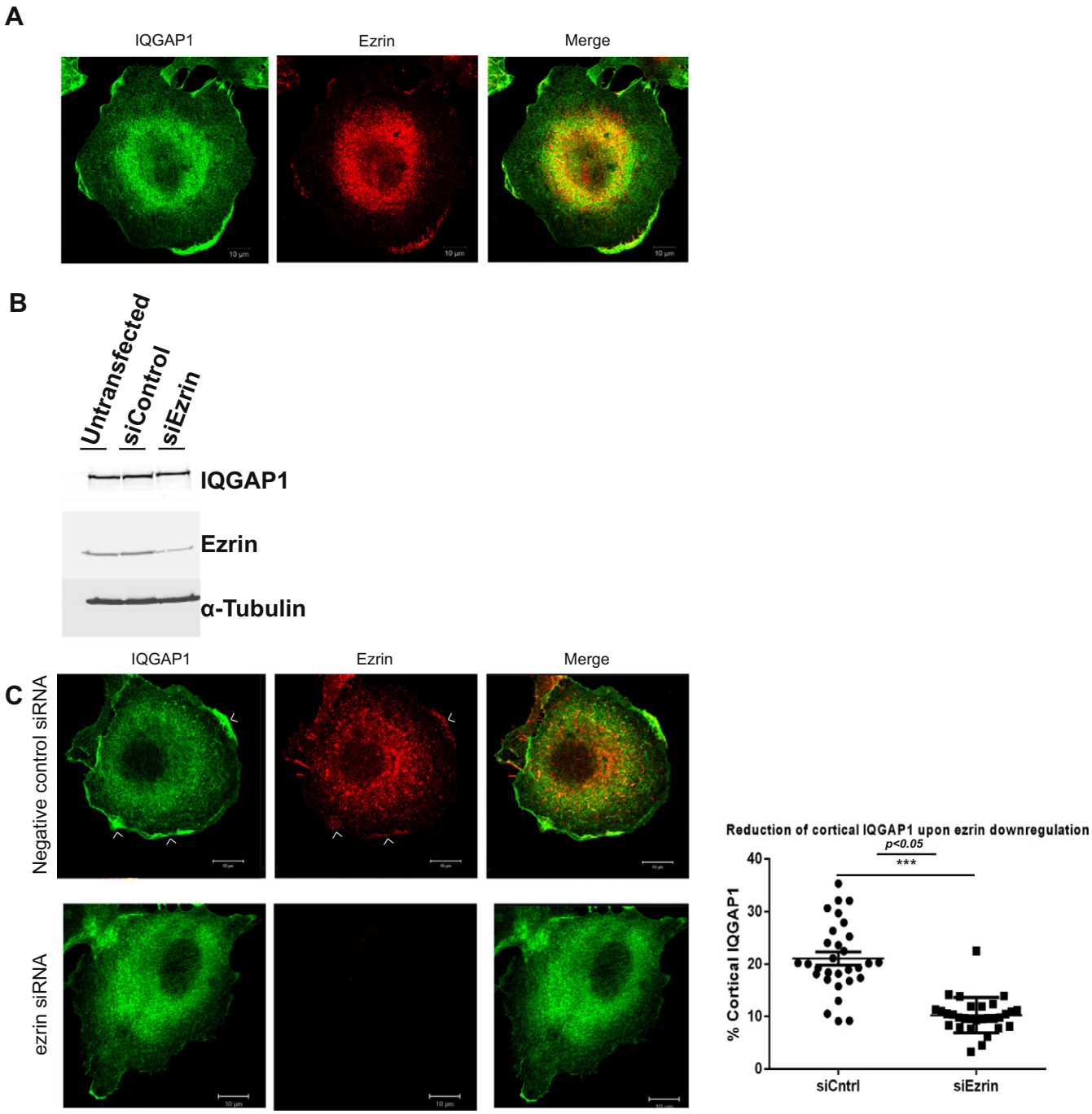

Fig. 7. Ezrin and IQGAP1 colocalize in ECV304 cells and the down regulation of ezrin reduces the cortical localization of IQGAP1. A. Ezrin and IQGAP1 colocalize in ECV304 cells and are enriched in the cell cortex. After fixation and permeabilization, cells were stained with polyclonal antibodies against human IQGAP1 (*green channel*) and monoclonal antibodies against human ezrin (*red channel*) followed by appropriate fluorescently labeled secondary antibodies. Scale bars, 10 μm. B. Western blot analysis of ECV304 cells transfected with control or ezrin siRNA. Blots were stained with polyclonal anti-ezrin (1:5000), monoclonal anti-IQGAP1 (1:5000) and anti-α-tubulin (1: 10,000) (loading control) antibodies. Note that the expression levels of IQGAP1 remain unaffected upon ezrin downregulation. C (left). Representative confocal images of IQGAP1 and ezrin staining in siControl-transfected and ezrin down-regulated ECV304 cells. White arrowheads denote the co-enrichment of IQGAP1 and ezrin in the cortex of control transfected cells. Note the reduction in cortical IQGAP1 signal upon ezrin depletion. C (right), Quantification of cortical IQGAP1 in control and ezrin depleted cells. n = 30 cells in control as well as ezrin depleted conditions. ***, $P < 0.05$. Error bars represent SEM.

4. Concluding remarks

The multidomain protein IQGAP1 is a scaffolding protein in the submembranous cytoskeleton that has been shown to function in several signaling pathway by recruiting signaling intermediates through direct interactions and thereby providing a close proximity required for efficient signal transduction (for review see [16]). Signaling-competent molecules assembled by IQGAP1 include Rho protein family members that act in organizing actin dynamics and intermediates of the MEK/ERK signal transduction pathway. Here we show that IQGAP1 can also bind an important structural protein of the cortical cytoskeleton, the membrane-F-actin linker ezrin. Thereby regulators of actin organization such as Cdc42 and Rac1 can be placed in close proximity to where actin filaments dock at the plasma membrane enabling a tight spatial control of actin dynamics directly at the plasma membrane.

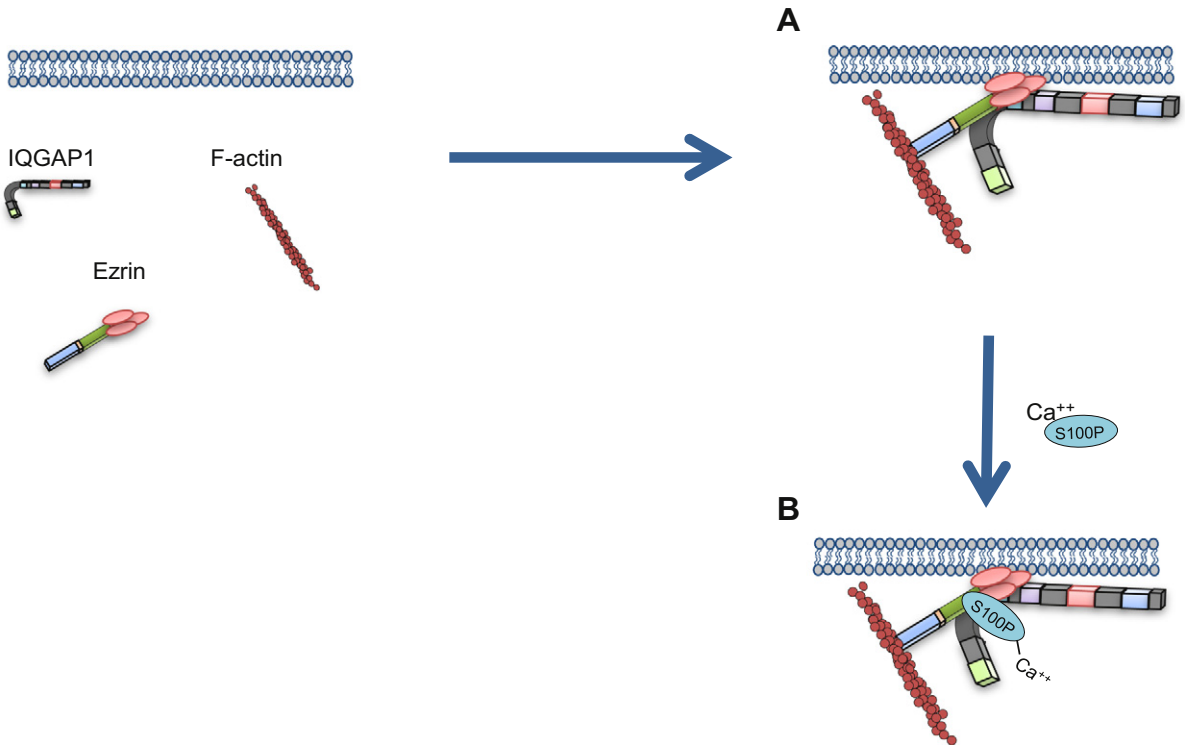

Fig. 8. Schematic illustration of the IQGAP1/ezrin/S100P complex formations. Non-phosphorylated ezrin that is bound to the plasma membrane in unstimulated cells via PI(4,5)P_2 binding could recruit IQGAP1 to the cell cortex. Upon an intracellular Ca^{2+} rise which could result from growth factor stimulation, Ca^{2+} bound S100P could be directed to such IQGAP1/ezrin complexes. This could result in further recruitment of ezrin and IQGAP1 and/or stabilization of the ezrin–IQGAP1 interaction thereby contributing to the coordinated regulation of cortical cell dynamics.

Acknowledgments

We thank Kozo Kaibuchi (University of Nagoya, Japan) for providing SF9 cells expressing full-length IQGAP1 and for anti-IQGAP1 antibodies. This work has been supported by the Deutsche Forschungsgemeinschaft (DFG GE 514/8-1, 9-1).

References

[1] G. Salbreux, G. Charras, E. Paluch, Actin cortex mechanics and cellular morphogenesis, Trends Cell Biol. 22 (2012) 536–545.
[2] L. Jiang, J.M. Phang, J. Yu, S.J. Harrop, A.V. Sokolova, A.P. Duff, K.E. Wilk, H. Alkhamici, S.N. Breit, S.M. Valenzuela, L.J. Brown, P.M.G. Curmi, CLIC proteins, ezrin, radixin, moesin and the coupling of membranes to the actin cytoskeleton: a smoking gun? Biochim. Biophys. Acta 1838 (2014) 643–657.
[3] M. Schmick, P.I.H. Bastiaens, The interdependence of membrane shape and cellular signal processing, Cell 156 (2014) 1132–1138.
[4] I. de Curtis, J. Meldolesi, Cell surface dynamics — how Rho GTPases orchestrate the interplay between the plasma membrane and the cortical cytoskeleton, J. Cell Sci. 125 (2012) 4435–4444.
[5] A.J. Ridley, Life at the leading edge, Cell 145 (2011) 1012–1022.
[6] J. Saarikangas, H. Zhao, P. Lappalainen, Regulation of the actin cytoskeleton–plasma membrane interplay by phosphoinositides, Physiol. Rev. 90 (2010) 259–289.
[7] R. Wollman, T. Meyer, Coordinated oscillations in cortical actin and Ca2$^+$ correlate with cycles of vesicle secretion, Nat. Cell Biol. 14 (2012) 1261–1269.
[8] R. Donato, B. Cannon, G. Sorci, F. Riuzzi, K. Hsu, D. Weber, C. Geczy, Functions of S100 proteins, Curr. Mol. Med. 13 (2013) 24–57.
[9] L. Santamaria-Kisiel, A.C. Rintala-Dempsey, G.S. Shaw, Calcium-dependent and -independent interactions of the S100 protein family, Biochem. J. 396 (2006) 201–214.
[10] C.W. Heizmann, G. Fritz, B.W. Schäfer, S100 proteins: structure, functions and pathology, Front. Biosci. a J. Virtual Libr. 1 (2002) 1356–1368.
[11] M. Koltzscher, C. Neumann, S. König, V. Gerke, Ca2$^+$-dependent binding and activation of dormant ezrin by dimeric S100P, Mol. Biol. Cell 14 (2003) 2372–2384.
[12] A. Heil, A.R. Nazmi, M. Koltzscher, M. Poeter, J. Austermann, N. Assard, J. Baudier, K. Kaibuchi, V. Gerke, S100P is a novel interaction partner and regulator of IQGAP1, J. Biol. Chem. 286 (2011) 7227–7238.
[13] A.L. Neisch, R.G. Fehon, Ezrin, radixin and moesin: key regulators of membrane–cortex interactions and signaling, Curr. Opin. Cell Biol. 23 (2011) 377–382.
[14] R.G. Fehon, A.I. McClatchey, A. Bretscher, Organizing the cell cortex: the role of ERM proteins, Nat. Rev. Mol. Cell Biol. 11 (2010) 276–287.
[15] J. Austermann, A.R. Nazmi, C. Müller-Tidow, V. Gerke, Characterization of the Ca2$^+$-regulated ezrin–S100P interaction and its role in tumor cell migration, J. Biol. Chem. 283 (2008) 29331–29340.
[16] C.D. White, H.H. Erdemir, D.B. Sacks, IQGAP1 and its binding proteins control diverse biological functions, Cell. Signal. 24 (2012) 826–834.
[17] D.T. Brandt, R. Grosse, Get to grips: steering local actin dynamics with IQGAPs, EMBO Rep. 8 (2007) 1019–1023.
[18] A. Ruiz-Sáenz, L. Kremer, M. a Alonso, J. Millán, I. Correas, Protein 41R regulates cell migration and IQGAP1 recruitment to the leading edge, J. Cell Sci. 124 (2011) 2529–2538.
[19] J. Liu, J.J. Guidry, D.K. Worthylake, Conserved sequence repeats of IQGAP1 mediate binding to ezrin, J. Proteome Res. 13 (2014) 1156–1166.
[20] G.O. Mbele, J.C. Deloulme, B.J. Gentil, C. Delphin, M. Ferro, J. Garin, M. Takahashi, J. Baudier, The zinc- and calcium-binding S100B interacts and co-localizes with IQGAP1 during dynamic rearrangement of cell membranes, J. Biol. Chem. 277 (2002) 49998–50007.
[21] G. Wang, S. Zhang, D.G. Fernig, D. Spiller, M. Martin-fernandez, H. Zhang, Y. Ding, Z. Rao, P.S. Rudland, R. Barraclough, Heterodimeric interaction and interfaces of S100A1 and S100P, 3832004. 375–383.
[22] T. Isobe, N. Ishioka, T. Okuyama, Structural Relation of Two S-100 Proteins in Bovine Brain; Subunit Composition of S-100a Protein, 4741981. 469–474.
[23] V. Niggli, C. Andréoli, C. Roy, P. Mangeat, Identification of a phosphatidylinositol-4,5-bisphosphate-binding domain in the N-terminal region of ezrin, FEBS Lett. 376 (1995) 172–176.
[24] J. Braunger, B.R. Brückner, S. Nehls, A. Pietuch, V. Gerke, I. Mey, A. Janshoff, C. Steinem, Phosphatidylinositol 4,5-bisphosphate alters the number of attachment sites between ezrin and actin filaments: a colloidal probe study, J. Biol. Chem. 289 (2014) 9833–9843.